Electronic Supplementary Material (ESI) for Physical Chemistry Chemical Physics.

Quantitative analysis of cross-talk in partly deuterated samples of nuclear spins hyperpolarized by dynamic nuclear polarization (DNP) in the thermal mixing regime: Supplementary Information

Bogdan A. Rodin[1,2,3], Vineeth Francis Thalakottoor Jose Chacko[1], Mathieu Baudin[1,4], Nicolas Birilirakis[1], Geoffrey Bodenhausen[1], Alexandra V. Yurkovskaya[2,3], and Daniel Abergel[1]

[1]Laboratoire des biomolécules, LBM, Département de chimie, Ecole normale supérieure,PSL University, Sorbonne Université, CNRS, 75005 Paris, France.
[2]International Tomography Center, Siberian Branch of the Russian Academy of Science, Novosibirsk 630090, Russia
[3]Physics Department, Novosibirsk State University, Novosibirsk, 630090, Russia
[4]Laboratoire de Chimie et Biochimie Pharmacologiques et Toxicologiques Université Paris Cité 145, Rue des Saints Pères 75006, Paris, France
[†]Email: phagost@gmail.com, daniel.abergel@ens.psl.eu

April 6, 2023

1 Comparison of spin temperatures of the nuclear spins at maximum polarization

The spin temperatures at the end of build-up are shown for the different nuclei present in the sample in Figure 1. These temperatures are identical, or almost so. For the ^{31}P experiments, the maximal spin temperature was compared to the ^{1}H nuclei.

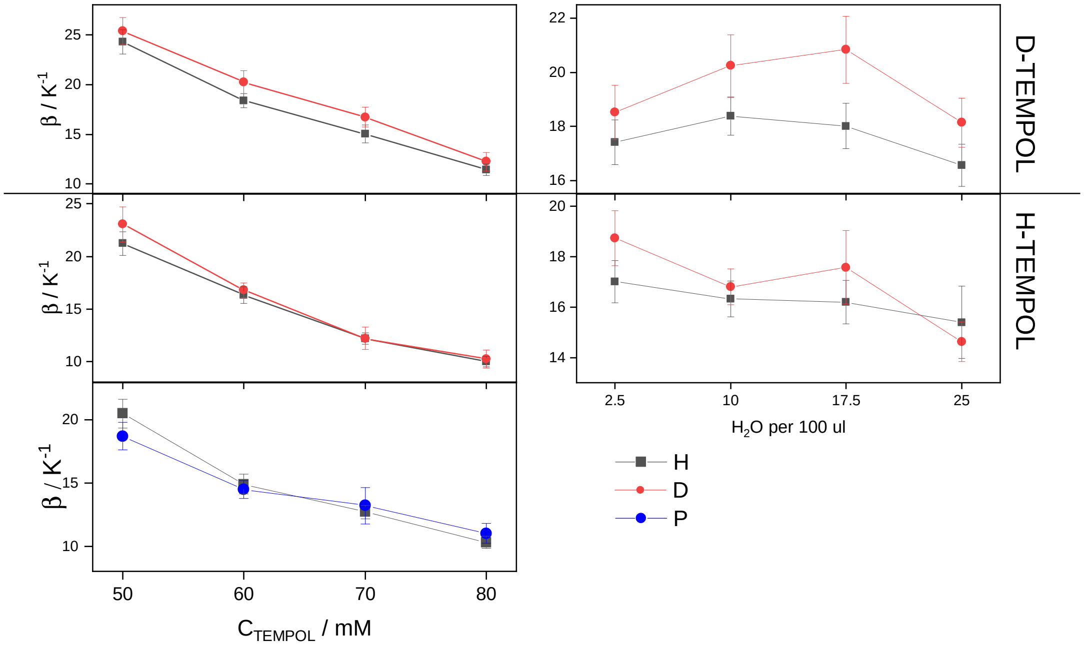

Figure 1 The inverse spin temperaturs β at the end of build-up for different nuclei.

2 Spin temperature error estimation

The errors may be estimated by a standard uncertainty propagation:[1]

$$\Delta\beta = \sqrt{\sum_i \left(\frac{\partial\beta}{\partial x_i}\Delta x_i\right)^2}, \tag{1}$$

where Δx_i is the error estimation of the independent variable. In our case, these variables are the inverse temperature b_0, the hyperpolarized signal S and the thermal signal S_0. Their errors were estimated in the following way:

- $\Delta b_0 = \Delta T/T_0^2$, where the temperature error was estimated to be ±0.1
- ΔS was estimated by integrating over the noise region with the same interval and then calculating std
- ΔS_0 was estimated by fitting with bi-exponential function the repolarization experiments with other nuclei saturation

2.1 Spin-1/2 derivatives

The process of derivative calculation is quite straightforward, here we present the final result only.

$\partial\beta_S/\partial S$	$\frac{2k_B}{\hbar\omega_0}\frac{P(\beta_0)}{S_0}(1-\left[\frac{SP(\beta_0)}{S_0}\right]^2)^{-1}$
$\partial\beta_S/\partial S_0$	$\frac{2k_B}{\hbar\omega_0}\frac{SP(\beta_0)}{S_0^2}(1-\left[\frac{SP(\beta_0)}{S_0}\right]^2)^{-1}$
$\partial\beta_S/\partial\beta_0$	$\frac{S}{S_0}(1-\left[\frac{SP(\beta_0)}{S_0}\right]^2)^{-1}\cosh^{-2}\left(\frac{\hbar\omega_0\beta_0}{2k_B}\right)$

2.2 Spin-1 derivatives

Using the fact that $(f^{-1})'(x) = 1/f'[f^{-1}(x)]$, and the fact that:

$$B'(x) = 2\mathrm{sh}\frac{3x}{2}\left(2\mathrm{sh}\frac{x}{2}\mathrm{ch}x + \mathrm{sh}x\left[\mathrm{ch}\frac{x}{2} - 3\mathrm{sh}\frac{x}{2}\coth\frac{3x}{2}\right]\right), \tag{2}$$

where sh means sinh and ch means cosh, one could get all the derivatives for spin-1:

$\partial\beta_S/\partial S$	$\frac{k_B}{\hbar\omega_0}\frac{B(\beta_0)}{S_0}(B'\{B^{-1}[\frac{S}{S_0}B(\beta_0)]\})^{-1}$
$\partial\beta_S/\partial S_0$	$\frac{k_B}{\hbar\omega_0}\frac{SB(\beta_0)}{S_0^2}(B'\{B^{-1}[\frac{S}{S_0}B(\beta_0)]\})^{-1}$
$\partial\beta_S/\partial\beta_0$	$\frac{S}{S_0}(B'\{B^{-1}[\frac{S}{S_0}B(\beta_0)]\})^{-1}B'(\beta_0)$

3 Pulse correction of the fitting procedure

To perform pulse correction, we have modified the differential equation solver of the scipy python package (function odeint) to handle discrete events. Between pulses, the evolution is propagated by Provotorv's equation using the python odeint function. The pulse modifies the inverse temperature value according to:

$$\begin{aligned} \beta' &= \beta\cos\theta, && \text{for } {}^1\mathrm{H}, {}^{31}\mathrm{P} \\ \beta' &= \beta\cos\theta_1\cos\theta_2, && \text{for } {}^2\mathrm{H}. \end{aligned}$$

Two different pulse angles are used for ^{2}H because the two-pulse echo sequence was used to detect the nuclei.

Additionally. the steady state may be affected by excessive pulsing. In our case, this effect was mostly significant in the 31P repolarization experiments (see Figure 2(a)), where rather large excitation pulses (4°) were used. This, however, was not the case in depolarization experiments that were performed with small, 1°, excitation angles. Indeed, in case of too frequent pulse monitoring of the signal the spins reach a steady state instead of the thermal polarization. This is taken into account through the following correction procedure. For pulse angle θ, time interval τ between pulses, and relaxation time T towards thermal equilibrium, the signals for FIDs n and $n+1$ are related according to:

$$S_{n+1} = S_{\mathrm{eq}} + (S_n\cos\theta - S_{\mathrm{eq}})\exp(-\tau/T) \tag{3}$$

Therefore, in steady-state, one has:

$$S' = S_{\mathrm{eq}}f, \quad \text{where} \quad f = \frac{1-\exp(-\tau/T)}{1-\cos\theta\exp(-\tau/T)} \tag{4}$$

Thus, data can be corrected by simply multiplying them by f, with $T = \tau_p$, the decay rate constant of 31P signal. The result is shown in figure 2(b). Such corrections were also performed for deuterium data, where the cosine in Eq. 4 is substituted by $\cos\theta_1\cos\theta_2$ (two angles were used for small-angle quadrupolar spin-echo). It is worth noting that this strategy works correvctly for heteronuclei that have decay rates equal to τ_X. This is not the case of 1H, but because only small angles were used, and due to the fast relaxation rates, the steady state was not significantly affected.

The differential evolution algorithm previously used for finding the global minimum becomes too time-consuming for this approach when using the modified native python function modified by ourselves, so that we used the following two-step minimization strategy:

- find the best fit using a differential evolution algorithm without accounting for the excitation angle (this turned out to provide best-fit parameters very close to the final values);
- the final parameter search was performed by the fast Levenberg-Marquardt algorithm, taking into account the pulses, with parameters of the previous step as starting values.

We give here details about the experiments using a 60 mM H-TEMPOL concentration and 10 microlitres of additional water. This case is illustrative of all other experiments, and a comparison between fits obtained with the previous and the pulse-corrected models are shown in Figure 3 One can see that the corrected solver better predicts the behaviour almost in the same fashion, were steady-state data correction accounts for smaller repolarization maxima in 2H case. In the case of 1H, no change is observed. The parameters for the previous and present fitting procedures are shown in Table 1. It is noteworthy that the parameter values obtained in both cases are almost identical, except for τ_D, which takes somewhat larger values for the pulse-corrected model. This observation is common to all the performed experiments.

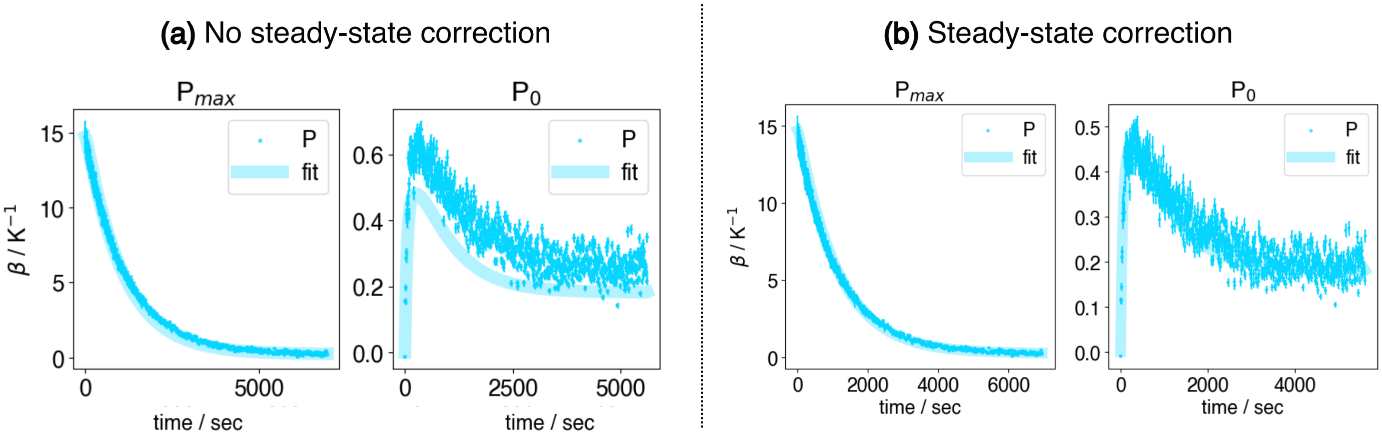

Figure 2 The result of fitting the 31P data for 60 mM TEMPOL sample (a) with pulse correction but without steady-state correction, (b) with both pulse correction and without steady-state correction

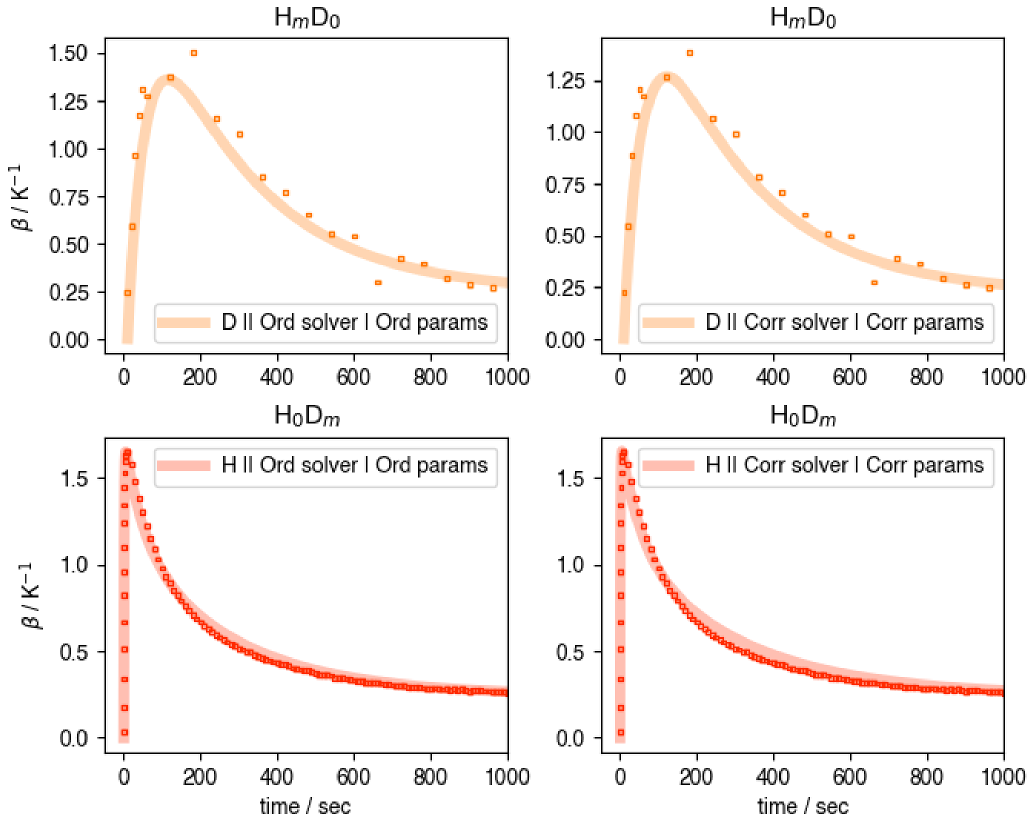

Figure 3 The comparison of the fitted curves obtained by the fit using the standard Provotorov model("ord" solver and "ord" params) or the pulse-corrected one ("corr" solver and "corr" params).

Table 1 The comparison of the obtained parameters of the Provotorov equations between a pulse-corrected and uncorrected fitting protocols.

60 mM H-TEMPOL, 10 % v/v H_2O

Method	τ_H / s	τ_H^u / s	τ_D / s	τ_{NZ} / s	f^u	f	χ_R^2
no pulse correction	3.21	0.80	**253**	3.1	0.04	0.09	1.84
pulse corrected	3.26	0.66	**276**	3.2	0.04	0.08	1.74

4 Three reservoir model fittings

4.0.1 Fitting results

The figures in this section show the fitting results of the buildup curves for the three-reservoir model described in the article.

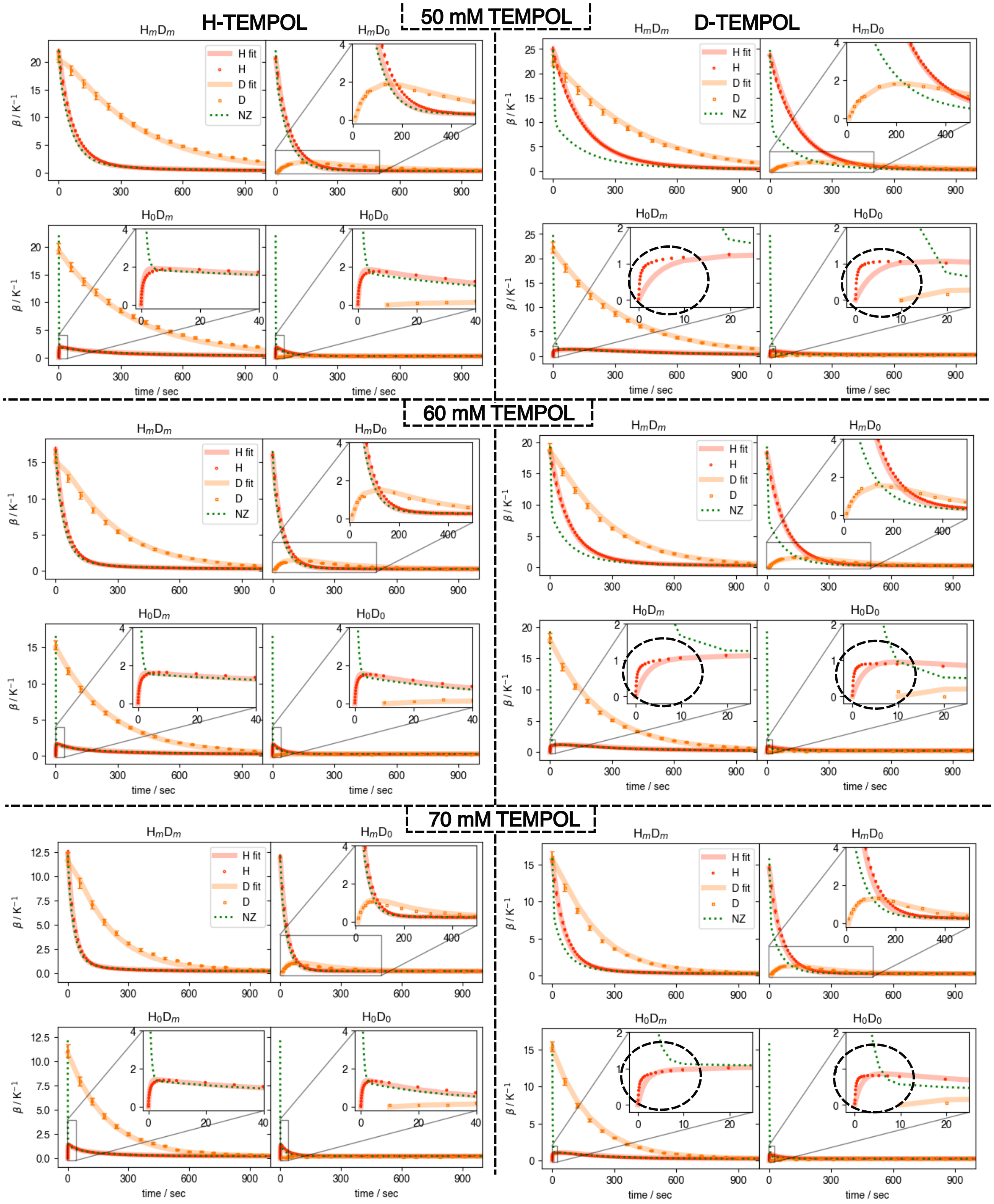

Figure 4 Fitting results of the cross-talk buildup curves for the three-reservoir model, for protonated and deutarated TEMPOL at 50, 60 and 70 mM and 1:4:5 H_2O:D_2O:glycerol-d8.

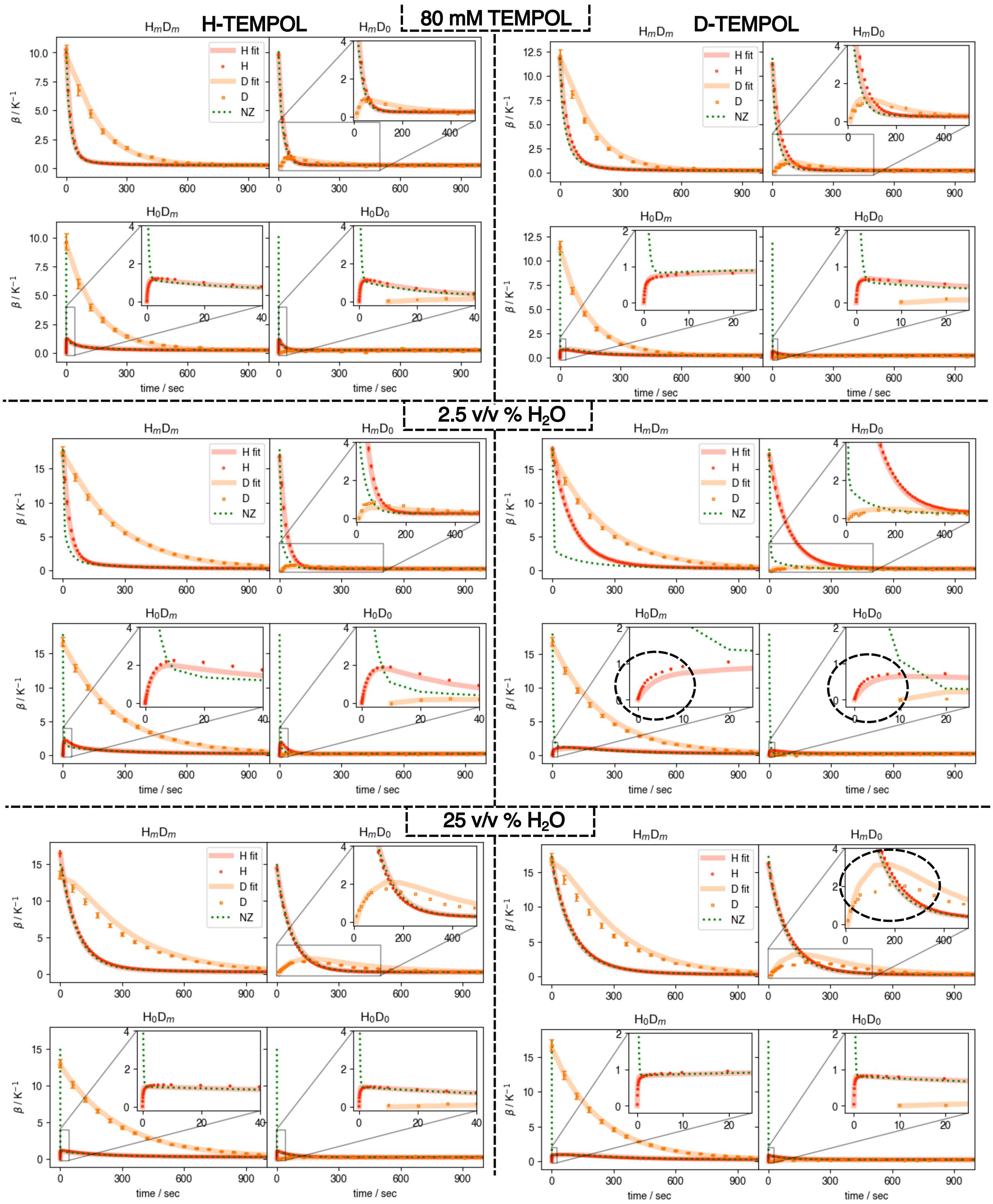

Figure 5 The fitting results for 3 reservoir model for cross-talk experiments for protonated and deutarated TEMPOL with the sample composition 80 mM TEMPOL 1:4:5 H_2O:D_2O:glycerol-d8, as well as 60 mM TEMPOL 2.5:47.5:50 and 25:25:50 H_2O:D_2O:glycerol-d8

4.0.2 Correlations between model parameters

The significant correlations for the three-reservoir model are presented in table 2. Representative examples of parameter correlation diagrams for 50 and 60 mM TEMPOL (protonated and deuterated) are shown in Figure 6. All diagrams may be found on the github page.[2] Mind the change of notations on the graph axes: $\tau_1 \rightarrow \tau_H$, $\tau_2 \rightarrow \tau_D$, $\tau_{nz} \rightarrow \tau_{NZ}$, and f1 corresponds to f.

Table 2 The significant correlation for the three reservoirs model

H-TEMPOL

C_{TEMPOL}, mM	Significant correlations ($>$ 0.4)
50	$c(\tau_{NZ}, f) = 0.94$, $c(\tau_H, f) = 0.70$, $c(\tau_H, \tau_{NZ}) = 0.56$
60	$c(\tau_{NZ}, f) = 0.94$, $c(\tau_H, f) = 0.57$, $c(\tau_H, \tau_{NZ}) = 0.42$
70	$c(\tau_{NZ}, f) = 0.93$, $c(\tau_H, f) = 0.56$, $c(\tau_H, \tau_{NZ}) = 0.44$
80	$c(\tau_{NZ}, f) = 0.84$, $c(\tau_H, f) = 0.57$
H_2O v/v, %	
2.5	None
10	$c(\tau_{NZ}, f) = 0.94$, $c(\tau_H, f) = 0.57$, $c(\tau_H, \tau_{NZ}) = 0.42$
25	$c(\tau_{NZ}, f) = 0.95$, $c(\tau_H, f) = 0.42$

D-TEMPOL

C_{TEMPOL}, mM	Significant correlations ($>$ 0.4)
50	$c(\tau_{NZ}, f) = 0.85$, $c(\tau_H, f) = 0.65$
60	$c(\tau_{NZ}, f) = 0.86$, $c(\tau_H, f) = 0.71$
70	$c(\tau_{NZ}, f) = 0.87$, $c(\tau_H, f) = 0.80$, $c(\tau_H, \tau_{NZ}) = 0.49$
80	$c(\tau_{NZ}, f) = 0.92$, $c(\tau_H, f) = 0.83$, $c(\tau_H, \tau_{NZ}) = 0.68$
H_2O v/v, %	
2.5	None
10	$c(\tau_{NZ}, f) = 0.86$, $c(\tau_H, f) = 0.71$
25	$c(\tau_{NZ}, f) = 0.95$, $c(\tau_D, \tau_{NZ}) = -0.84$, $c(\tau_D, f) = -0.43$

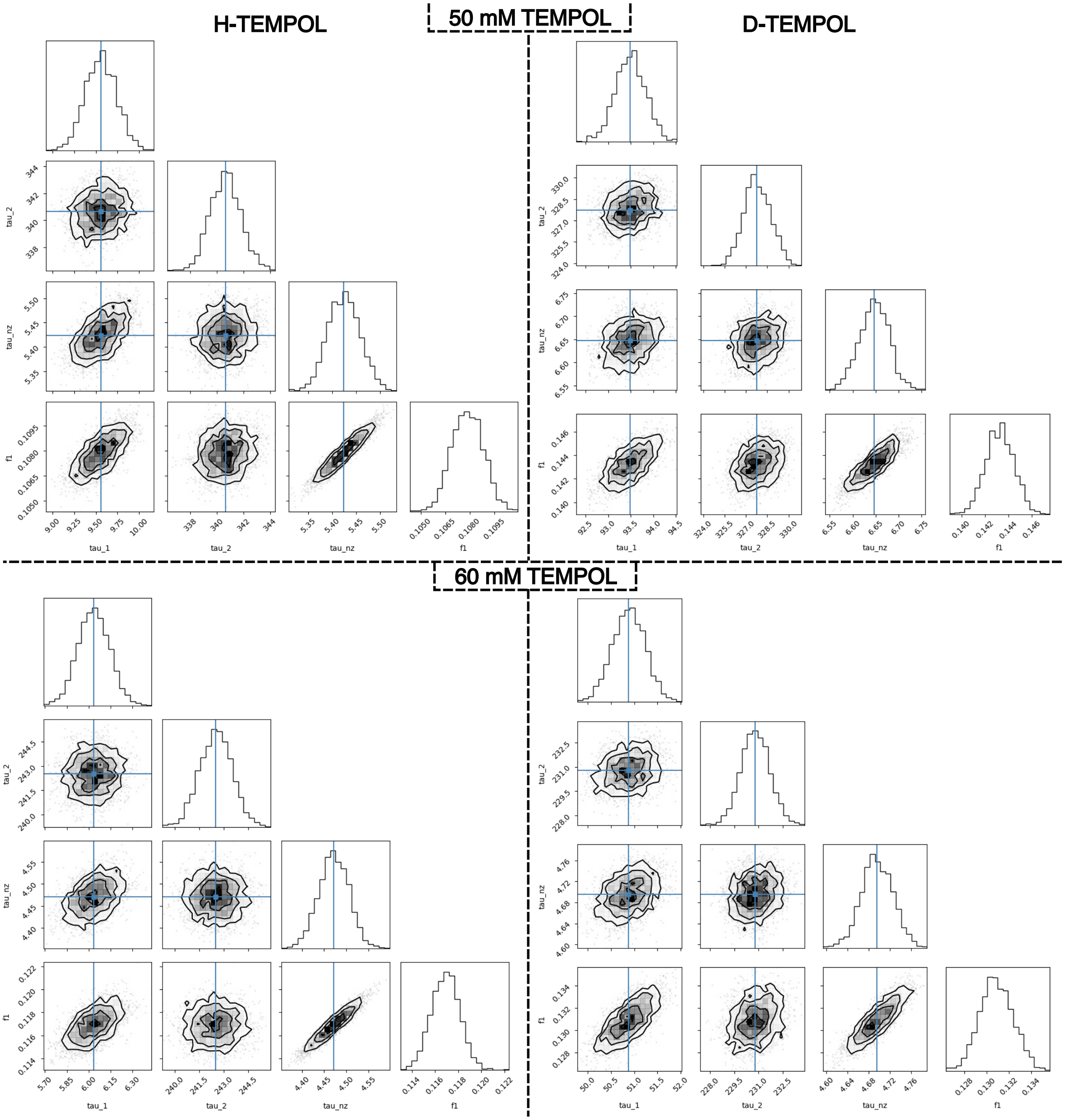

Figure 6 Cross-talk experiments with a 3-reservoir model for protonated and deuterated TEMPOL with samples containing 50 and 60 mM TEMPOL, 1:4:5 by volume of H_2O:D_2O:glycerol-d8.

5 Four reservoir model fittings

Figures in this section correspond to the four-reservoir model described in the article.

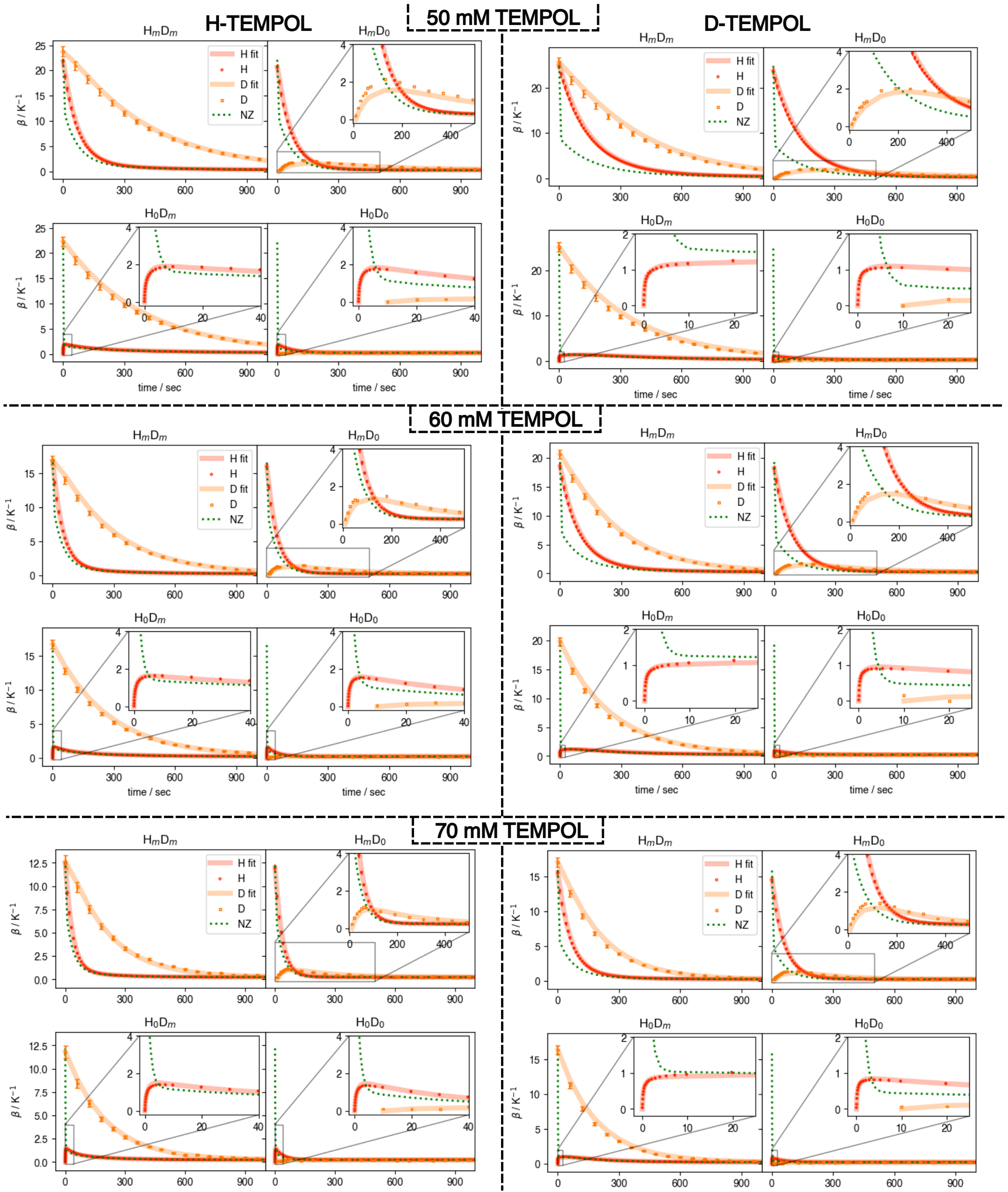

Figure 7 The fitting results for 4 reservoir model for cross-talk experiments for protonated and deutarated TEMPOL with the sample composition 50, 60 and 70 mM TEMPOL, 1:4:5 H_2O:D_2O:glycerol-d8.

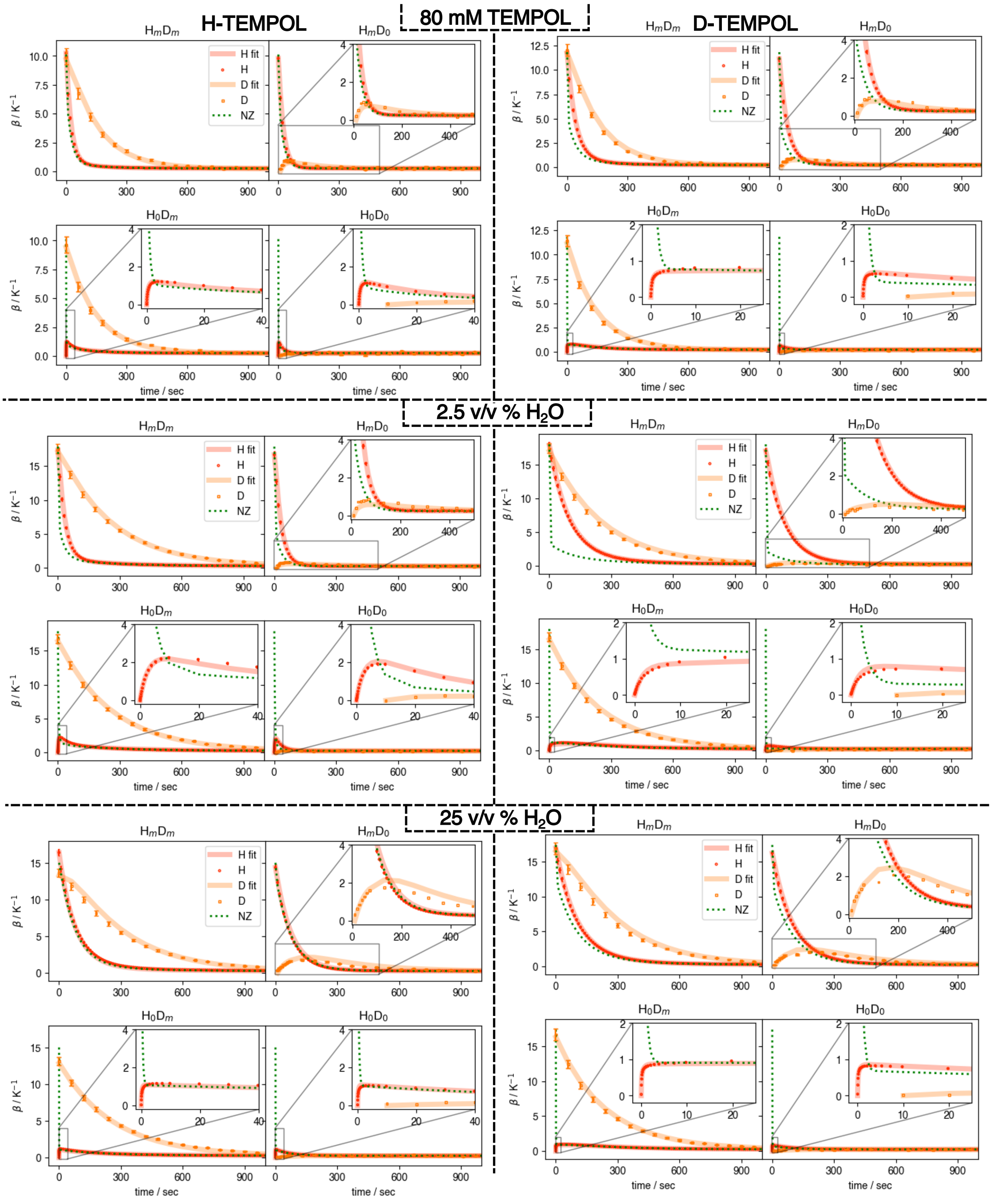

Figure 8 Fits for cross-talk experiments with a 3-reservoir model for protonated and deutarated TEMPOL with samples containing 80 mM TEMPOL and 1:4:5 by volume of H2O:D2O:glycerol-d8, as well as 60 mM TEMPOL and 2.5:47.5:50 and 25:25:50 by volume of H_2O:D_2O:glycerol-d8

5.0.1 Correlations

The most significant correlation graphs for the four-reservoir model are presented in table 3. Correlation diagrams for 60 mM TEMPOL (protonated and deuterated) are shown in Figure 9. All diagrams may be found on the github page.[2] Mind the change of notations: $\tau_1 \rightarrow \tau_H$, $\tau_2 \rightarrow \tau_D$, $\tau_{nz} \rightarrow \tau_{NZ}$, and f1 corresponds to f.

Table 3 The significant correlation for the three reservoirs model

H-TEMPOL	
C_{TEMPOL}, mM	Significant correlations (> 0.7)
50	c(τ_{NZ}, f) = 0.97, c(τ^u_H, f^u) =0.85, c(τ_{NZ}, f^u) = -0.82, c(f, f^u) = -0.77
60	c(τ_{NZ}, f) = 0.98, c(τ^u_H, f^u) = 0.85, c(τ_{NZ}, f^u) = -0.82, c(f, f^u) = -0.83
70	c(τ_{NZ}, f) = 0.95, c(τ_{NZ}, f^u) = -0.84, c(f, f^u) = -0.76, c(τ^u_H, f^u) = 0.74
80	c(τ_{NZ}, f) = 0.95, c(τ_{NZ}, f^u) = -0.91, c(f, f^u) = -0.83, c(τ^u_H, f^u) =0.75, c(τ_H, f^u) = 0.74
H_2O v/v, %	
2.5	c(τ_{NZ}, f) = 0.98, c(τ_{NZ}, f^u) = -0.94, c(τ^u_H, f^u) =0.93, c(f, f^u) = -0.92, c(τ_H, f^u) = 0.91, c(τ^u_H, τ_{NZ}) = -0.88, c(τ^u_H, f) = -0.82, c(τ_H, τ_{NZ}) = -0.81, c(f, τ_H) = -0.82, c(τ^u_H, τ_H) = 0.74
10	c(τ_{NZ}, f) = 0.98, c(τ^u_H, f^u) = 0.85, c(τ_{NZ}, f^u) = -0.82, c(f, f^u) = -0.83
25	c(τ_{NZ}, f) = 0.98, c(τ_{NZ}, f^u) = -0.97, c(f, f^u) = -0.95, c(τ^u_H, f^u) =0.93, c(τ_H, f^u) = 0.88, c(τ^u_H, τ_{NZ}) = -0.87, c(τ^u_H, f) = -0.85, c(τ_H, τ_{NZ}) = -0.85, c(f, τ_H) = -0.83, c(τ^u_H, τ_H) = 0.73
D-TEMPOL	
C_{TEMPOL}, mM	Significant correlations (> 0.7)
50	c(τ_{NZ}, f) = 0.99, c(τ^u_H, f^u) = 0.94, c(τ_{NZ}, f^u) = -0.86, c(f, f^u) = -0.84, c(τ^u_H, τ_{NZ}) = -0.75
60	c(τ_{NZ}, f) = 0.98, c(τ^u_H, f^u) = 0.90, c(τ_{NZ}, f^u) = -0.86, c(f, f^u) = -0.85, c(τ^u_H, τ_{NZ}) = -0.74
70	c(τ_{NZ}, f) = 0.98, c(τ_{NZ}, f^u) = -0.90, c(τ^u_H, f^u) = 0.90, c(f, f^u) = -0.89, c(τ^u_H, τ_{NZ}) = -0.77, c(τ^u_H, f) = -0.7
80	c(τ_{NZ}, f) = 0.98, c(τ_{NZ}, f^u) = -0.91, c(f, f^u) = -0.87, c(τ^u_H, f^u) = 0.84, c(τ^u_H, τ_{NZ}) = -0.73
H_2O v/v, %	
2.5	c(τ_{NZ}, f) = 0.99, c(τ^u_H, f^u) = 0.74, c(τ^u_H, τ_{NZ}) = -0.73, c(τ_{NZ}, f^u) = -0.72, c(f, f^u) = -0.71, c(τ^u_H, f) = -0.7
10	c(τ_{NZ}, f) = 0.98, c(τ^u_H, f^u) = 0.90, c(τ_{NZ}, f^u) = -0.86, c(f, f^u) = -0.85, c(τ^u_H, τ_{NZ}) = -0.74
25	c(τ_{NZ}, f) = 0.99, c(τ_{NZ}, f^u) = -0.89, c(f, f^u) = -0.87

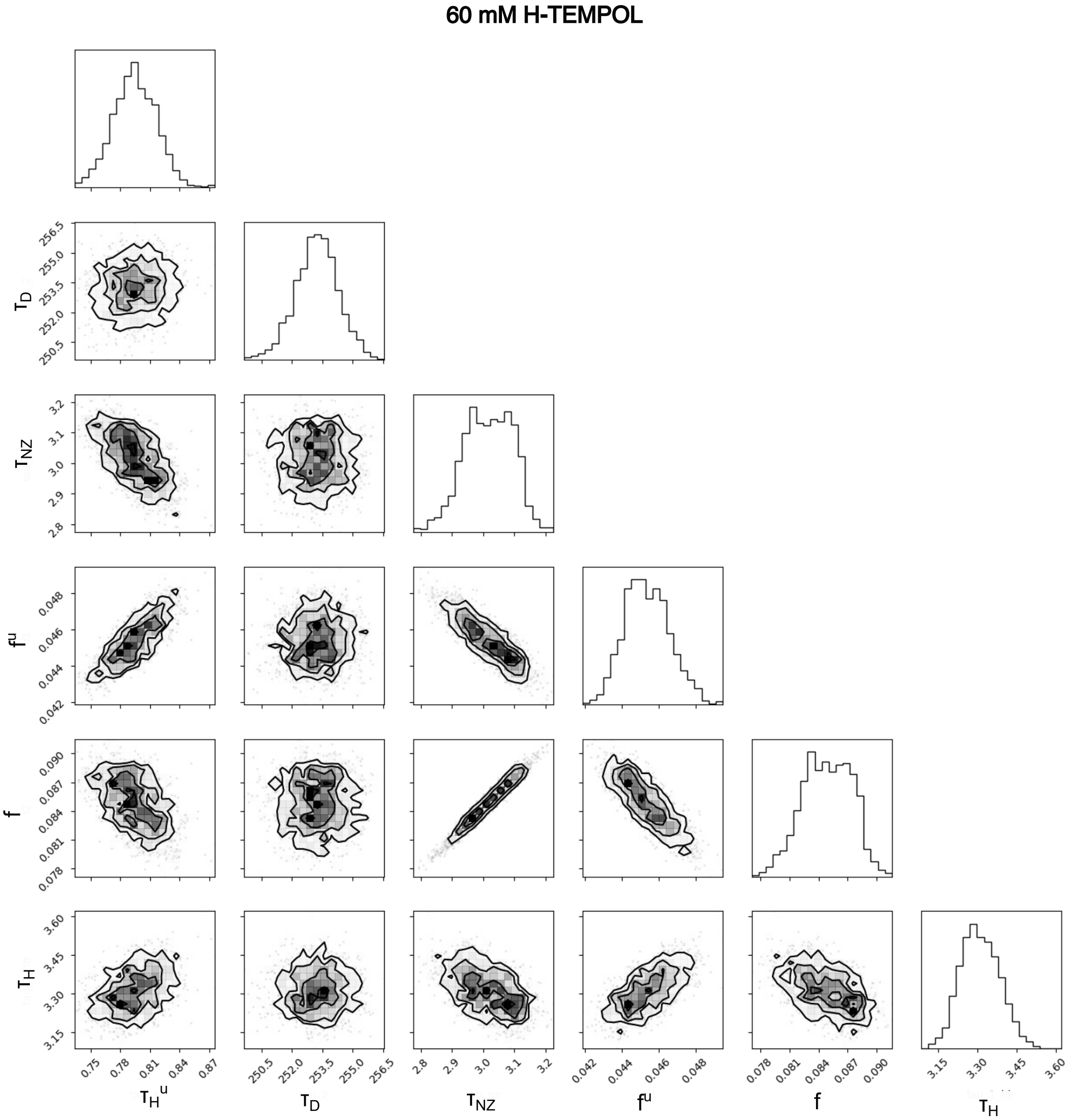

Figure 9 The correlation diagram for 4 reservoir model for cross-talk experiments for protonated TEMPOL with the sample composition of 60 mM H-TEMPOL, 1:4:5 H_2O:D_2O:glycerol-d8.

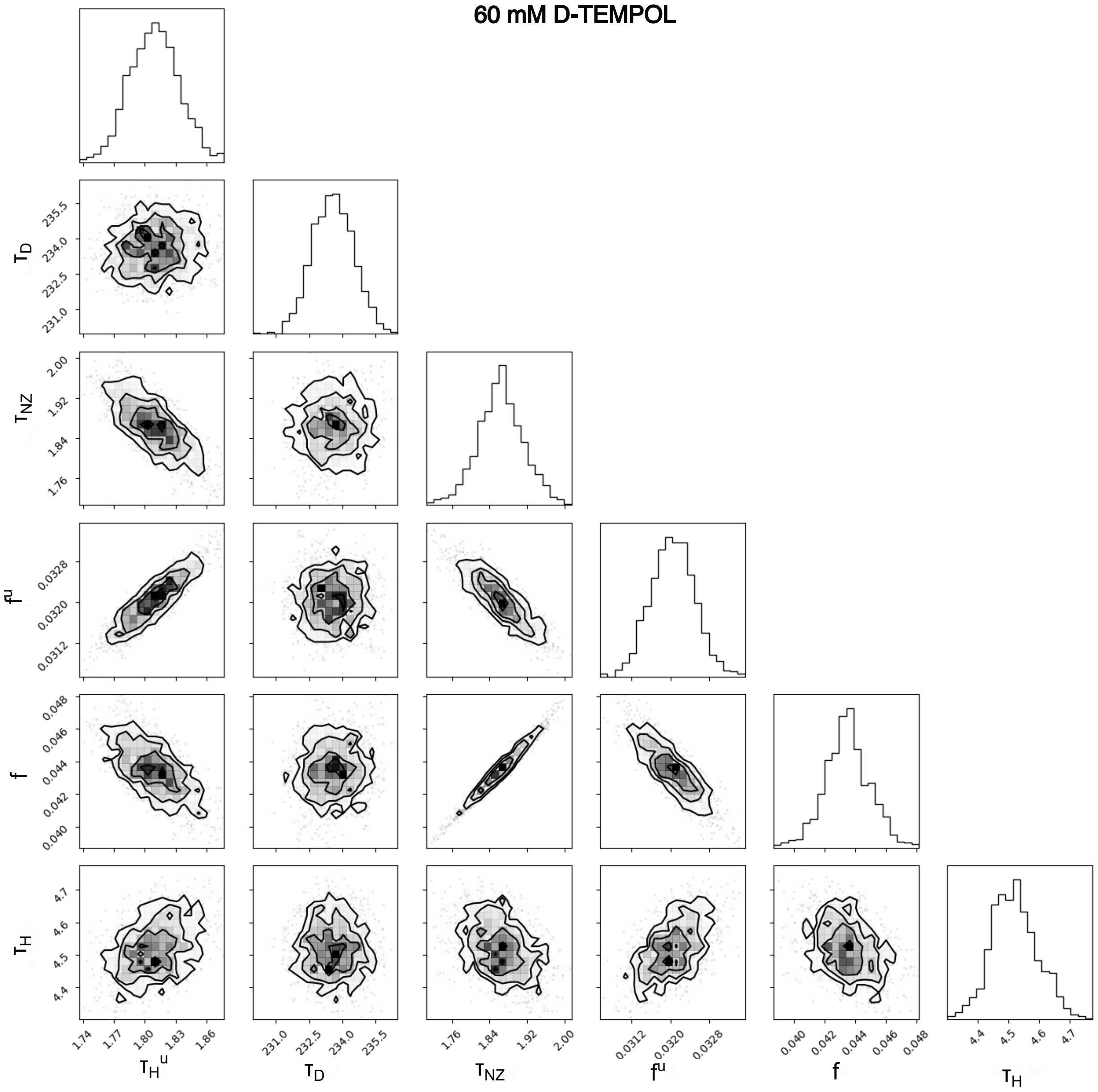

Figure 10 Cross-talk experiments with a 4-reservoir model for deuterated TEMPOL with a sample containing 60 mM D-TEMPOL, 1:4:5 by volume H_2O:D_2O:glycerol-d8.

6 Simulation of the size of the hidden reservoir

The simulation was performed as in ref.[3] by counting the fractions of spins having greater paramagnetic shift than a given value. The assumption is that the shift experienced by a single proton due to the paramagnetic shift originating from several electrons adds up. So, the paramagnetic shift experienced by a proton at position $\vec{r}_j$ is calculated as:

$$\Delta\omega_{\text{para}}(\vec{r}_j) = \frac{\mu_0}{4\pi}\frac{\hbar\gamma_e\gamma_n}{4}\sum_{k=1}^{N}\frac{1}{|\vec{r}_j-\vec{r}_k|^3}\left(1-3\left(\frac{r_{jz}-r_{kz}}{|\vec{r}_j-\vec{r}_k|}\right)^2\right) \tag{5}$$

Then, all the nuclei that have shifts larger than some threshold $|\Delta\omega_{\text{para}}| < \omega_n$ may be considered hidden. For example, this threshold may be considered as the saturation bandwidth of the pulse. It may work the other way around: for a given fraction of hidden spins one can extract the respective frequency, and then the radius. In our work, to estimate the radius, one considers the frequency shift to be on the order of RMS of the Larmor frequency shift corresponding to a single electro-nuclear spin-spin interaction:

$$\Delta\omega_{\text{RMS}} = \frac{1}{2\sqrt{5}}\frac{\mu_0}{4\pi}\frac{\hbar\gamma_e\gamma_n}{r^3} \tag{6}$$

To simulate the abovementioned, one computed the position of randomly distributed electrons in the cube of 40 nm with the number of electrons corresponding to the respective concentration. A random distribution of 1000 nuclear spins was computed (5 nm widths on the edges of the box are excluded). The paramagnetic shift and the PRE are computed for each nucleus by summing the contribution of all electrons, as detailed above, and repeated for 35 random electron configurations. The resulting curves are shown in Figure 11

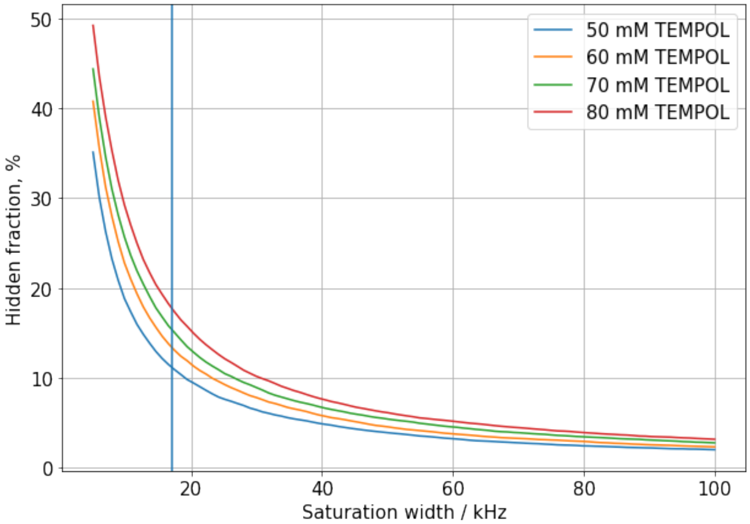

Figure 11 Computed hidden fraction due to the paramagnetic shift as a function of the nutation frequency of the pulse using the average of 35 electron configurations. The vertical line corresponds to 17 kHz saturation bandwidth, which was used in the current work.

7 X nucleus experimental data fitting

Fitting of the ^{31}P cross-talk experiments was performed for the three-reservoir model as described in the main text, with the addition of the ^{31}P inverse temperature equation. The parameters $c_{NZ,H,D}$ and $\tau_{NZ,H,D}$ were taken from the fits of the samples without ^{31}P nuclei, and only the $\tau_X == \tau_P$ parameter was fitted. This was justified by the fact that the heat capacity of ^{31}P is much smaller than ^{1,2}H and should not change the parameters significantly. For example, for the sample composition presented here (50, 60, 70, 80 mM H-TEMPOL, 0.5 M K_2HPO_4, 1:4:5 H_2O:D_2O:glycerol-d8), $c_P/c_{H,D} \approx 100$. The resulting fitted curves are shown in Figure12. The obtained τ_P values are $1503 \pm 4, 1120 \pm 2, 889 \pm 6, 604 \pm 5$ for 50, 60, 70, 80 mM H-TEMPOL concentrations respectively.

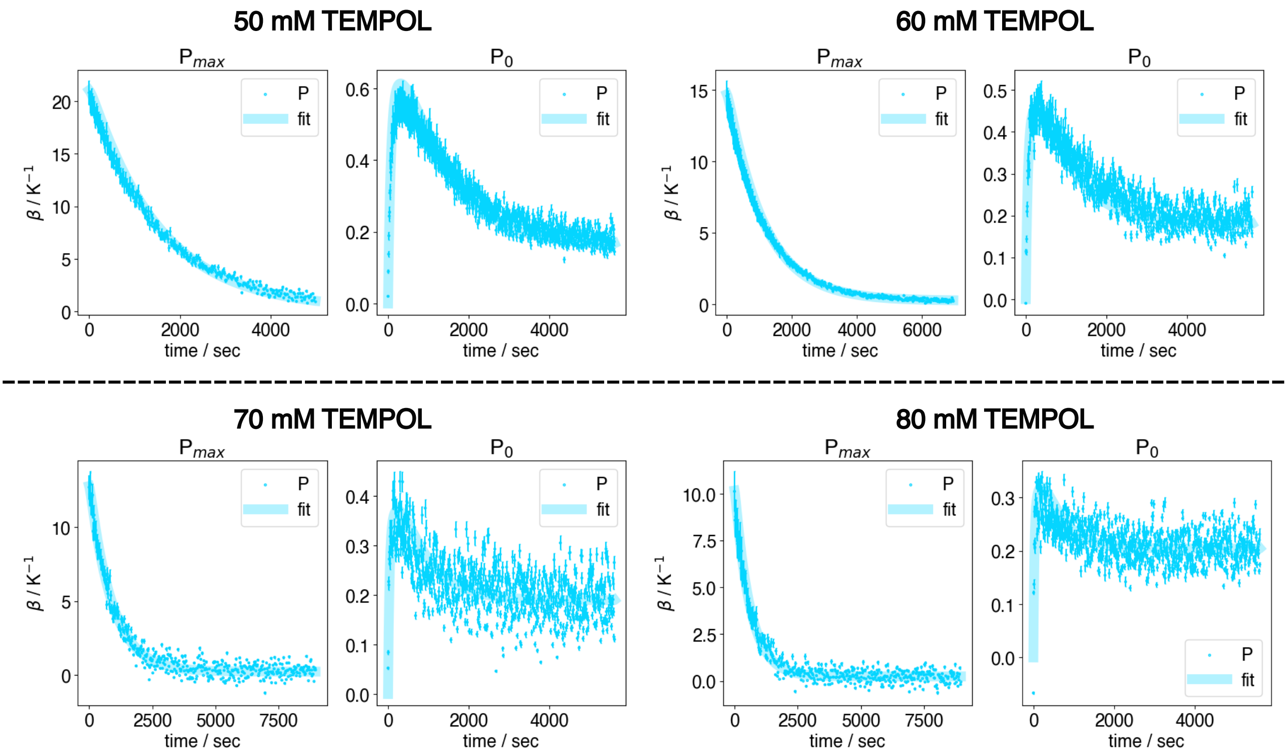

Figure 12 The fitting results for the 3 reservoir model for cross-talk experiments on the P nuclei only. The sample composition was 50, 60, 70, 80 mM H-TEMPOL, 0.5 M K_2HPO_4, 1:4:5 H_2O:D_2O:glycerol-d8.

8 Arbitrary angle spin-echo sequence for quadrupolar interaction refocusing in case of spin-1 calculated using SpinDynamica package

Quadrupolar spin echo for a small pulse angles at the low temperature approximation

In this notebook I would like to
see the form of the density matrix for D in the low-temperature approximation when the excitation and refocusing angle are small.

The density matrix for D may be written as :

$$\rho_{\mathrm{eq}}(x) = a(x)\ E + \frac{1}{2} B(x)\ \left(I_z + P(x)\ I_z{}^2\right)$$

where $x = \omega_0 / \mathrm{kT}$, and the coefficients are :

$$a(x) = \frac{\mathrm{Sinh}(x/2)}{\mathrm{Sinh}(3\,x/2)},\quad B(x) = \frac{\mathrm{Sinh}(x)\ \mathrm{Sinh}(x/2)}{\mathrm{Sinh}(3\,x/2)},\quad P(x) = \tanh(x/2)$$

The Hamiltonian should be the quadrupolar one and it equals to :

$$H_Q = \omega_Q\ \frac{1}{6}\ \left(3\ I_z{}^2 - 2\ E\right)$$

The pulse sequence should be something like :

$$\tau\ \text{--}\ \beta_1\ \text{--}\ \tau\ \text{--}\ \beta_2$$

Also, it seems there is some kind of
phase cycling sequence. I can also try to check it

Initialization

In[1]:=
```
Needs["SpinDynamica`"]
```

```
SpinDynamica version 3.3.1 loaded
```

```
SetUserLevel: The user level is being initialized to 2. The user level may be set to an integer between 1 and 3 by using
    SetUserLevel[level]. Low user levels provide strong syntax trapping at the expense of slow execution for some routines.
    High user levels relax the syntax trapping in order to provide better execution speeds.

SetUserLevel: The user level has been set to 2.

SetUserLevel: Additional definitions have been given to the following symbols:
    {Dot, Exp, Expand, Plus, Power, Simplify, Times, WignerD}
```

Set-up

```
In[2]:= SetSpinSystem[{{1, 1}}]

SetSpinSystem: the spin system has been set to {{1, 1}}

SetBasis: the state basis has been set to ZeemanBasis[{{1, 1}}, BasisLabels → Automatic].
```

Initial density matrix and helper functions

For future use, we will consider two cases of density matrix (high-temp and low-temp) separately.

The high-temp will be:

In[3]:=
$$\rho_{\mathrm{highT}} = \frac{1}{3}\,\mathtt{opI["z"]};$$

And the low-temp will be:

```
In[4]:= a[x_] := Sinh[x/2] / Sinh[3 x / 2];
        B[x_] := Sinh[x] Sinh[x/2] / Sinh[3 x / 2];
        P[x_] := Tanh[x/2];
```

In[7]:=
$$\rho_{\mathrm{lowT}} = \mathtt{B[x]} * \left(\mathtt{opI["z"]} + \mathtt{P[x]\ opI["z"].opI["z"]}\right);$$

One transforms into the other when the temp -> inf :
(here I don’t account for the identity matrix)

In[8]:=
$$\left(\mathtt{Series}[\rho_{\mathrm{lowT}},\ \{x,\ 0,\ 1\}]\ \mathtt{//\ Normal}\right) / x$$

Out[8]=
$$\frac{I_{1\,z}}{3}$$

So, everything good in this regard.

Quadrupolar Hamiltonian

In[9]:=
$$H_Q = \frac{\omega_Q}{6}\left(3\,\mathtt{opI["z"].opI["z"]} - 2\,\mathtt{UnityOperator[]}\right)$$

Out[9]=
$$\frac{1}{6}\,\omega_Q\left(3\,(I_{1\,z}\bullet I_{1\,z}) - 2\,\mathbb{1}\right)$$

Operators to express

The rotation superoperator

We will use two different rotation operators to see the effect of the first and the second excitation pulse.

In[10]:=
$$\mathtt{R[i\_,\ a\_]\ :=\ RotationSuperoperator[1,\ \{}\beta_i\mathtt{,\ a\}];}$$

See if we rotate

In[11]:=
```
R[1, "x"]@ρlowT
```

Out[11]=
$$\mathrm{Csch}\left[\frac{3\,x}{2}\right]\,\mathrm{Sinh}\left[\frac{x}{2}\right]\,\mathrm{Sinh}[x]\,\left(R_{1\,x}(\beta_1)\bullet I_{1\,z}\bullet R_{1\,x}(-\beta_1)+\left(R_{1\,x}(\beta_1)\bullet I_{1\,z}\bullet I_{1\,z}\bullet R_{1\,x}(-\beta_1)\right)\,\mathrm{Tanh}\left[\frac{x}{2}\right]\right)$$

The quadrupolar superoperator

Making the super operator for propagation under the quadrupolar evolution

First, the commutator superoperator that induces the evolution.

In[12]:=
```
CS = CommutationSuperoperator[HQ]
```

Out[12]=
$$\mathrm{CommutationSuperoperator}\left[\frac{1}{6}\,\omega_Q\,\left(3\,(I_{1\,z}\bullet I_{1\,z})-2\,\mathbb{1}\right)\right]$$

Then, let’s constract the final propogator

In[13]:=
```
U1 = Exp[-I t1 CS]
```

Out[13]=
$$e^{\mathrm{CommutationSuperoperator}\left[-\frac{1}{6}\,i\,t1\,\omega_Q\,(3\,(I_{1\,z}\bullet I_{1\,z})-2\,\mathbb{1})\right]}$$

The second unitary operator for the second pulse

In[14]:=
```
U2 = Exp[-I t2 CS]
```

Out[14]=
$$e^{\mathrm{CommutationSuperoperator}\left[-\frac{1}{6}\,i\,t2\,\omega_Q\,(3\,(I_{1\,z}\bullet I_{1\,z})-2\,\mathbb{1})\right]}$$

Coherent filtration superoperator

In[15]:=
```
P = CoherenceOrderFiltrationSuperoperator[-1]
```

Out[15]=
```
CoherenceOrderFiltrationSuperoperator[{{1}, {-1}}]
```

Small pulse angle approximation

Here I introduce the function to series the final expressions for a density matrix

In[16]:=
```
Ser[i_, x_] := (Series[#, {βi, 0, x}] // Normal) &
```

In[17]:=
```
Ser[1, 3]
```

Out[17]=
```
Normal[Series[#1, {β1, 0, 3}]] &
```

Final echo sequence

So, finally, let’s define the final small angle spin echo sequence. The problem is I am not sure about the phases, so we will figure them out in the process:

In[18]:=
```
SESeq [phase1_, phase2_] := P@U1@R[2, phase2]@U1@R[1, phase1]@# &
```

Cleaning from ω_Q terms:

To figure out if the sequence was successful or not, we should filter out all the terms in the resulted density matrix that doesn’t depend on the ω_Q. To do so, we are going to use the following magic:

In[19]:=
```
QFilter = Select[(# // Expand), FreeQ[#, ωQ] &] &
```

Out[19]=
```
Select[Expand[#1], FreeQ[#1, ωQ] &] &
```

In[20]:=
```
QSer[x_] := (FourierCoefficient[#, t1 ωQ / 2, x] // Normal) &
```

Some operators addition:

In[21]:=
```
InPhase = opI["-"]
AntiPhase = opI["-"].opI["z"] + opI["z"].opI["-"]
```

Out[21]= I_1^-

Out[22]= $I_1^- \bullet I_{1z} + I_{1z} \bullet I_1^-$

High temperature density matrix

Let’s check the resulted density matrix under the usual excitation:

In[23]:=
```
P@R[1, "x"]@ρhighT
```

```
SetOperatorBasis: the operator basis has been set to ShiftAndZOperatorBasis[{{1, 1}}, Sorted → CoherenceOrder].
```

Out[23]= $-\frac{1}{6}\, i\, I_1^- \,\mathrm{Sin}[\beta_1]$

And now let’s see what will happen under SESeq:

In[24]:=
```
ResHighT = SESeq["x", "y"]@ρhighT // Simplify
```

Out[24]=

$$\frac{1}{12}\Big(e^{-i\,t1\,\omega_Q}\left(-1+e^{i\,t1\,\omega_Q}\right)\left(I_1^-\bullet I_{1z}+I_{1z}\bullet I_1^-\right)\left(-i\left(1+e^{i\,t1\,\omega_Q}\right)\mathrm{Cos}[\beta_2]^2\,\mathrm{Sin}[\beta_1]+e^{\frac{1}{2}i\,t1\,\omega_Q}\,\mathrm{Cos}[\beta_1]\,\mathrm{Sin}[\beta_2]\right)+ I_1^-\Big(-i\,e^{-i\,t1\,\omega_Q}\left(1+e^{2\,i\,t1\,\omega_Q}\right)\mathrm{Cos}[\beta_2]^2\,\mathrm{Sin}[\beta_1]+ \mathrm{Sin}[\beta_2]\left(e^{-\frac{1}{2}i\,t1\,\omega_Q}\left(1+e^{i\,t1\,\omega_Q}\right)\mathrm{Cos}[\beta_1]-2\,i\,\mathrm{Sin}[\beta_1]\,\mathrm{Sin}[\beta_2]\right)\Big)\Big)$$

We should get the refocused matrix when the pulses are 90 degree:

In[25]:=
```
(ResHighT /. β2 → β1) /. β1 → π / 2
```

Out[25]= $-\frac{1}{6}\, i\, I_1^-$

Now let’s do some magic to see what terms are left after small angle excitation, and this terms should not depend on ω_Q:

In[26]:=
```
QFilter@ResHighT
```

Out[26]= $-\frac{1}{6}\, i\, I_1^- \,\mathrm{Sin}[\beta_1]\,\mathrm{Sin}[\beta_2]^2$

So, the sequence work in the low-temperature regime

Low temperature density matrix

Let’s repeat the same procedures for the low-temp density matrix.
After one arbitrary angle excitation pulse:

In[27]:=
```
P@R[1, "x"]@ρlowT
```

Out[27]=

$$-\frac{1}{2}\,i\,\text{Csch}\left[\frac{3x}{2}\right] I_1^- \,\text{Sin}[\beta_1]\,\text{Sinh}\left[\frac{x}{2}\right]\text{Sinh}[x] - \frac{1}{4}\,i\,\text{Csch}\left[\frac{3x}{2}\right]\left(I_1^-\bullet I_{1z} + I_{1z}\bullet I_1^-\right)\text{Sin}[2\beta_1]\,\text{Sinh}\left[\frac{x}{2}\right]\text{Sinh}[x]\,\text{Tanh}\left[\frac{x}{2}\right]$$

In the small angle approximation:

In[28]:=
```
Ser[1, 1]@P@R[1, "x"]@ρlowT
```

Out[28]=

$$-\frac{1}{2}\,i\,\beta_1\left(\text{Csch}\left[\frac{3x}{2}\right] I_1^-\,\text{Sinh}\left[\frac{x}{2}\right]\text{Sinh}[x] + \text{Csch}\left[\frac{3x}{2}\right]\left(I_1^-\bullet I_{1z}\right)\text{Sinh}\left[\frac{x}{2}\right]\text{Sinh}[x]\,\text{Tanh}\left[\frac{x}{2}\right] + \text{Csch}\left[\frac{3x}{2}\right]\left(I_{1z}\bullet I_1^-\right)\text{Sinh}\left[\frac{x}{2}\right]\text{Sinh}[x]\,\text{Tanh}\left[\frac{x}{2}\right]\right)$$

Let’s see in-phase contribution:

In[29]:=
```
(OperatorAmplitude[P@R[1, "x"]@ρlowT  → InPhase] // ExpToTrig // Simplify)
```

Out[29]=

$$-\frac{1}{2}\,i\,\text{Csch}\left[\frac{3x}{2}\right]\text{Sin}[\beta_1]\,\text{Sinh}\left[\frac{x}{2}\right]\text{Sinh}[x]$$

And anti-phase contribution:

In[30]:=
```
(OperatorAmplitude[P@R[1, "x"]@ρlowT  → AntiPhase] // ExpToTrig // Simplify)
```

Out[30]=

$$-\frac{1}{2}\,i\,\text{Csch}\left[\frac{3x}{2}\right]\text{Sin}[2\beta_1]\,\text{Sinh}\left[\frac{x}{2}\right]^3$$

This sequence is still quite hard to interpret.

Let’s see what we would get after the spin-echo sequence, but we will calculate it for all possible phases:

In[32]:=
```
Phases = {"x", "y", "-x", "-y"}
```

Out[32]=
```
{x, y, -x, -y}
```

In[34]:=
```
For[i = 1, i < 5, i++,
      For[j = 1, j < 5, j++,
            l1 = Phases[[i]];
            l2 = Phases[[j]];
            ResLowT[l1, l2] = SESeq[l1, l2]@ρlowT
        ];
 ];
```

Let’s see the {x, x} contribution:

In[37]:=
```
QFilter@(OperatorAmplitude[ResLowT["x", "x"] → InPhase]) // Simplify
```

Out[37]=
```
0
```

In[38]:=
```
QFilter@OperatorAmplitude[ResLowT ["x", "x"]  → AntiPhase] // Simplify
```

Out[38]=

$$\frac{1}{2}\,i\,\text{Csch}\left[\frac{3x}{2}\right]\text{Sin}[2\beta_1]\,\text{Sin}[\beta_2]^2\,\text{Sinh}\left[\frac{x}{2}\right]^3$$

So, in this case we account only for AntiPhase part.

Now, let’s see the difference if we use {x,y} contribution:

```
In[39]:= QFilter@(OperatorAmplitude[ResLowT["x", "y"] → InPhase]) // Simplify
```

Out[39]=
$$-\frac{1}{2}\,\mathbb{i}\,\mathrm{Csch}\left[\frac{3\,x}{2}\right]\,\mathrm{Sin}[\beta_1]\,\mathrm{Sin}[\beta_2]^2\,\mathrm{Sinh}\left[\frac{x}{2}\right]\,\mathrm{Sinh}[x]$$

```
In[40]:= QFilter@OperatorAmplitude[ResLowT ["x", "y"]  → AntiPhase] // Simplify
Out[40]= 0
```

Here, contrary, only y contribution is survived.

Now, let’s see what the phased cycling proposed by Diego (half of it, because there is no point to use the whole sequence)

```
In[42]:= DiegoCycle = QFilter@(-ResLowT["x", "x"] + ResLowT["x", "y"] )
```

Out[42]=
$$-\frac{1}{2}\,\mathbb{i}\,\mathrm{Csch}\left[\frac{3\,x}{2}\right]\,I_1^-\,\mathrm{Sin}[\beta_1]\,\mathrm{Sin}[\beta_2]^2\,\mathrm{Sinh}\left[\frac{x}{2}\right]\,\mathrm{Sinh}[x]\,-$$
$$\frac{1}{4}\,\mathbb{i}\,\mathrm{Csch}\left[\frac{3\,x}{2}\right]\,(I_1^-\bullet I_{1\,z})\,\mathrm{Sin}[2\,\beta_1]\,\mathrm{Sin}[\beta_2]^2\,\mathrm{Sinh}\left[\frac{x}{2}\right]\,\mathrm{Sinh}[x]\,\mathrm{Tanh}\left[\frac{x}{2}\right]\,-$$
$$\frac{1}{4}\,\mathbb{i}\,\mathrm{Csch}\left[\frac{3\,x}{2}\right]\,(I_{1\,z}\bullet I_1^-)\,\mathrm{Sin}[2\,\beta_1]\,\mathrm{Sin}[\beta_2]^2\,\mathrm{Sinh}\left[\frac{x}{2}\right]\,\mathrm{Sinh}[x]\,\mathrm{Tanh}\left[\frac{x}{2}\right]$$

```
In[43]:= OperatorAmplitude[DiegoCycle → InPhase]
```

Out[43]=
$$-\frac{1}{2}\,\mathbb{i}\,\mathrm{Csch}\left[\frac{3\,x}{2}\right]\,\mathrm{Sin}[\beta_1]\,\mathrm{Sin}[\beta_2]^2\,\mathrm{Sinh}\left[\frac{x}{2}\right]\,\mathrm{Sinh}[x]$$

```
In[44]:= OperatorAmplitude[DiegoCycle → AntiPhase]
```

Out[44]=
$$-\frac{1}{2}\,\mathbb{i}\,\mathrm{Csch}\left[\frac{3\,x}{2}\right]\,\mathrm{Sin}[2\,\beta_1]\,\mathrm{Sin}[\beta_2]^2\,\mathrm{Sinh}\left[\frac{x}{2}\right]^3$$

So, in this case we should see both inphase and antiphase contributions.

Notes and references

[1] H. H. Ku *et al.*, *Journal of Research of the National Bureau of Standards*, 1966, **70**, 263–273.

[2] B. A. Rodin, *Cross Talk Data and Fitting Procedure*, 2022, `https://github.com/phagost/cross_talk_fit`.

[3] Q. Stern, S. F. Cousin, F. Mentink-Vigier, A. C. Pinon, S. J. Elliott, O. Cala and S. Jannin, *Science Advances*, 2021, **7**, eabf5735.